

# Pedestrian-level wind environment near a square-shaped super-tall building in various urban-like settings

A. U. Weerasuriya<sup>1</sup>, Xuelin Zhang<sup>2</sup>, Bin Lu<sup>3</sup>, K. T. Tse<sup>4</sup>

<sup>1</sup>Hong Kong Metropolitan University, Ho Man Tin, Hong Kong, [auweeras@hkmu.edu.hk](mailto:auweeras@hkmu.edu.hk)

<sup>2</sup>Sun Yat-sen University, Zhuhai, Guangdong, P.R. China, [zhangxlin25@mail.sysu.edu.cn](mailto:zhangxlin25@mail.sysu.edu.cn)

<sup>3</sup>City University of Hong Kong, Kowloon Tong, Hong Kong, [binlu4-c@my.cityu.edu.hk](mailto:binlu4-c@my.cityu.edu.hk)

<sup>4</sup>Hong Kong University of Science and Technology, Kowloon, Hong Kong, [timktse@ust.hk](mailto:timktse@ust.hk)

## SUMMARY

The pedestrian-level wind environment (PLWE) near super-tall buildings, buildings taller than 300 m, is less understood compared to wind effects on them. The PLWE near a square-shaped super-tall building in 14 different urban-like settings is evaluated using three-dimensional, steady-state, Reynolds-averaged Navier-Stokes (3D RANS) equation-based computational fluid dynamics (CFD) simulations. The characteristics of PLWEs, such as maximum normalized mean wind speed ratio ( $K_{max}$ ) and percentage areas of high and low wind speed ( $A_{HWS}$  and  $A_{LWS}$ ), are investigated with respect to a set of design parameters, including frontal area ratio ( $\lambda_f$ ), street aspect ratio ( $SR$ ), uniformity of building height, and building arrangement of the urban settings. The results show a positive correlation between  $K_{max}$  and  $SR$ ,  $\lambda_f$  of the surroundings with uniform height buildings and advantages of adopting staggered arrangement to alleviate intense wind flows in urban areas. Nonuniform-height buildings in a staggered arrangement effectively reduce  $K_{max}$  and eliminate  $A_{HWS}$  but have less effect in modifying  $A_{LWS}$ .

*Keywords: pedestrian-level wind environment, super-tall building, computational fluid dynamics simulation*

## 1. INTRODUCTION

The pedestrian-level wind environment (PLWE) near super-tall buildings is less understood compared to wind effects on them (Tamura et al. 2012; Tanaka et al. 2012, 2013). The extant knowledge is mainly attributed to studies such as Xu et al. (2017), who have evaluated the PLWE near a super-tall building with conventional (e.g., square, rectangular, circular, elliptical) and unconventional configurations (e.g., setback, tapered, inclined). In addition, Zhang et al. (2020a, b) have investigated pedestrian wind environments and wind comfort near a super-tall building with many of these configurations in a regular urban area in strong and weak wind climates.

The studies on isolated super-tall buildings and those in regular urban areas do not provide many details about the combined effect of a super-tall building and its surroundings on PLWE. Many parameters of the surrounding buildings, such as frontal area ratio ( $\lambda_f$  = ratio of building frontal area to ground surface area), plan area ratio ( $\lambda_p$  = ratio of building plan area to ground surface area), street aspect ratio ( $SR$  = ratio of building height to street width), non-uniform building heights, building arrangements can influence PLWE in an urban area (Razak et al., 2013). This study aims to investigate how these features affect the PLWE near a square-shaped super-tall building in various urban-like settings using computational fluid dynamics (CFD) simulation.

## 2. CFD SIMULATION

### 2.1. A Super-tall Building in Urban-like Settings

Urban-like settings contain a square-shaped super-tall building (height = 400 m, width = 50 m, depth = 50 m) at the centre of a group of medium-rise buildings (Figure 1). The medium-rise buildings have a plan area of 50 m  $\times$  50 m and three different heights: 50 m, 75 m, and 100 m. The buildings are arranged in regular, staggered, and mixed arrays with 50 m wide roads spanning longitudinal and lateral wind directions. These configurations result in a constant  $\lambda_p$  of 0.25,  $\lambda_f = 0.25, 0.375, 0.50$ , and  $SR = 1, 1.5, 2$  for 50 m, 75 m, and 100 m height buildings.

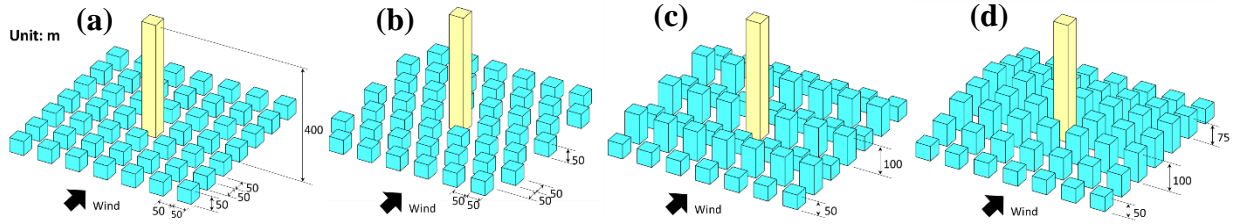


**Figure 1.** (a) 50 m regular, (b) 50 m staggered, (c) 50 m-100 m regular, (d) 50 m-75 m-100 m regular urban settings

### 2.2. Computational Settings and Parameters

The CFD simulations in this study were carried out as three-dimensional steady-state Reynolds-averaged Navier-Stokes equations-based (3D RANS) simulations using ANSYS FLUENT v.19.2 software. The buildings were modelled at a reduced scale of 1:500, similar to the wind tunnel tests (Xu et al., 2017) and previous CFD simulations (Zhang et al., 2020a,b). The computational domain has  $3H$  upstream and lateral lengths and  $10H$  downstream lengths from the edge of the building group, and a height of  $4H$ , where  $H$  is the height of the super-tall building. The domain was discretized into small hexahedral cells using the surface-grid extrusion technique. The first cell height above the ground,  $y_H$ , was more than twice the sand-grain equivalent roughness ( $k_s = 0.00074$  m). The ground was modelled as a rough surface using the standard wall function, and all building surfaces were smooth walls. The profiles of mean wind speed ( $U$ ), turbulent kinetic energy ( $k$ ), and turbulent kinetic energy dissipation rate ( $\epsilon$ ) were provided at the inlet, similar to those used in Zhang et al. (2020a,b). The realizable  $k$ - $\epsilon$  turbulence model was employed for the CFD simulations. The SIMPLE algorithm was used for pressure-velocity coupling, and pressure interpolation was of second order. The convection and viscous terms in the governing equations were solved using second-order discretization schemes. The results were considered converged when the iteration residuals had reached  $10^{-6}$  for continuity and  $10^{-7}$  for other variables and showed no further change with the number of iterations.

A grid sensitivity analysis was carried out comparing normalized mean wind speed ratio ( $K = U_{2m}/U_{2m,ambient}$ ) at the pedestrian level (2 m in full scale) in three different grids: Coarse, Intermediate, and Fine with 2,134,272, 3,905,164, and 5,916,736 cells, respectively. It was found that the Intermediate mesh had the lowest root-mean-squared-error (RMSE = 0.147) with respect to the Fine mesh; therefore, it was used for the CFD simulations. A grid arrangement similar to Intermediate mesh was employed for the validation test, which replicated the PLWE near a tall building in a regular urban area as in a wind tunnel test conducted by the Architectural Institute of Japan (Yoshie et al., 2007). In the validation test, CFD simulations displayed similar trends in  $K$  to the wind tunnel test data. Still, they had large deviations (up to 35%) at locations with weak wind circulation, while discrepancy was found to be less than 20% under high wind speeds.

### 3. RESULTS AND DISCUSSION

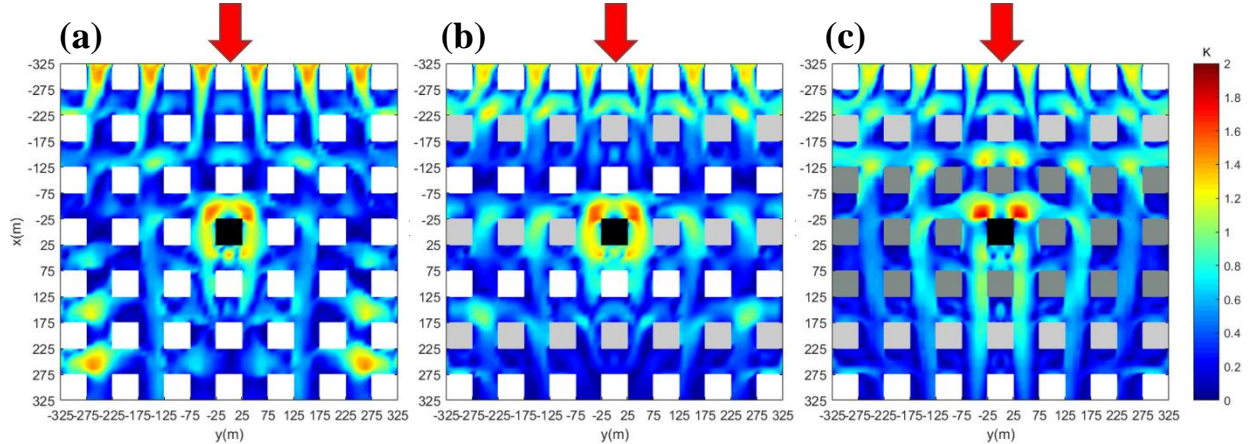


**Figure 2.** The distribution of  $K$  in a regular arrangement of (a) 50 m, (b) 50 m-75 m, (c) 50 m-75 m-100 m buildings ( $\square$  - 50 m,  $\square$  - 75 m,  $\square$  - 100 m,  $\blacksquare$  - 400 m height building)

Figure 2 shows the distribution of  $K$  in three urban settings: 50 m, 50 m-100 m, and 50 m-75 m-100 m buildings in a regular arrangement. The distributions of  $K$  show noticeable differences in the three building arrangements owing to variations in wind speed, location and size of the area with high and low wind speeds. Here, high and low wind speeds are arbitrarily defined as wind flows with  $K > 1.3$  and  $K < 0.7$ , respectively. Based on this definition, the area of high and low wind speed is calculated and expressed as a percentage of area:  $A_{HWS}$  and  $A_{LWS}$  with respect to the interrogated site of  $650 \text{ m} \times 650 \text{ m}$ . Large regions with elevated  $K$  are found near the super-tall building and upstream and lateral sides of taller buildings in regular arrangements (Figure 2). On the contrary, a significant portion of the downstream area of taller buildings in staggered arrangements is covered with lower  $K$  values (results are not shown here).

**Table 1.** Design parameters,  $K_{max}$ ,  $A_{HWS}$ , and  $A_{LWS}$  of 14 urban-like settings

Configuration	$\lambda_p$	$\lambda_f$	SR	$K_{max}$	$A_{HWS}$	$A_{LWS}$
50 m regular	0.25	0.25	1	1.531	2.85%	77.89%
50 m staggered	0.25	0.25	1	1.425	1.38%	80.30%
75 m regular	0.25	0.375	1.5	1.637	2.95%	77.47%
75 m staggered	0.25	0.375	1.5	1.495	1.39%	82.75%
100 m regular	0.25	0.50	2	1.775	4.65%	69.45%
100 m staggered	0.25	0.50	2	1.609	3.79%	81.28%
50 m-75 m regular	0.25	0.302	1&1.5	1.572	1.31%	76.61%
50 m-75 m staggered	0.25	0.302	1&1.5	1.300	0.10%	78.94%
50 m-100 m regular	0.25	0.354	1&2	1.468	0.84%	74.13%
50 m-100 m staggered	0.25	0.354	1&2	1.388	0.22%	80.19%
75 m-100 m regular	0.25	0.427	1.5&2	1.639	1.93%	80.81%
75 m-100 m staggered	0.25	0.427	1.5&2	1.462	0.42%	83.74%
50 m-75 m-100 m regular	0.25	0.390	1-2	1.799	0.79%	72.63%
50 m-75 m-100 m staggered	0.25	0.390	1-2	1.253	0%	78.98%

Table 1 shows design parameters:  $\lambda_p$ ,  $\lambda_f$ , and SR of 14 urban-like settings and maximum normalized wind speed ratio ( $K_{max}$ ),  $A_{HWS}$ , and  $A_{LWS}$  in respective PLWEs. Note that  $\lambda_f$  is the average value for the urban settings with different-height buildings. Several relationships between the design parameters and the statistics in PLWEs can be inferred; for instance, there is a positive correlation among  $\lambda_f$ , SR and  $K_{max}$  for uniform-height buildings in both regular and staggered arrangements. Moreover,  $K_{max}$  of regular arrangements is always larger than that of the staggered counterpart,

suggesting that the latter arrangement is advantageous in controlling  $K_{max}$  near a super-tall building. However, higher  $K_{max}$  does not necessarily imply larger  $A_{HWS}$ ; for example,  $A_{HWS}$  of 100 m staggered arrangement (3.79%) is larger than that of 75 m regular arrangement (2.95%) despite the  $K_{max}$  of the latter (1.637) being higher than the former (1.609). If non-uniform-height buildings are in the surrounding, then  $A_{HWS}$  in the interrogated area decreases more compared to  $K_{max}$ , while  $A_{LWS}$  remains approximately similar in the surroundings with uniform and nonuniform-height buildings. Strikingly, the 50 m-75 m-100 m staggered arrangement records the lowest  $K_{max}$  (1.253) and has no area of high wind speed ( $A_{HWS} = 0$ ).

## 5. CONCLUSIONS

This study investigated the PLWE near a square-shaped super-tall building in 14 different urban-like settings to correlate the magnitude of wind speed and areas of high and low wind speeds with design parameters of the urban settings. Two design parameters:  $\lambda_f$  and  $SR$ , of surroundings with uniform-height buildings positively correlate with  $K_{max}$ , but  $K_{max}$  and  $A_{HWS}$  display no strong interrelationship in many cases. The staggered building arrangement is advantageous in controlling the magnitude of maximum wind speed, whereas those with nonuniform-height buildings alleviate both the intensity and size of the area of high wind speeds. However,  $A_{LWS}$  is found to be less insensitive to the design parameters tested in this study.

## ACKNOWLEDGEMENTS

The work described in this paper was partially supported by the grants from the National Natural Science Foundation of China (No. 42175180) and a Theme-based research project T22-504/21R from the Research Grants Council (RGC) of the HKSAR, China.

## REFERENCES

- Razak, A.A., Hagishima, A., Ikegaya, N. and Tanimoto, J., 2013. Analysis of airflow over building arrays for assessment of urban wind environment. *Building and Environment*, 59, pp.56-65.
- Tamura, Y., Tanaka, H., Ohtake, K., Nakai, M. and Kim, Y., 2010. Aerodynamic characteristics of tall building models with various unconventional configurations. In *Structures Congress 2010* (pp. 3104-3113).
- Tanaka, H., Tamura, Y., Ohtake, K., Nakai, M. and Kim, Y.C., 2012. Experimental investigation of aerodynamic forces and wind pressures acting on tall buildings with various unconventional configurations. *Journal of Wind Engineering and Industrial Aerodynamics*, 107, pp.179-191.
- Tanaka, H., Tamura, Y., Ohtake, K., Nakai, M., Kim, Y.C. and Bandi, E.K., 2013. Aerodynamic and flow characteristics of tall buildings with various unconventional configurations. *International Journal of High-Rise Buildings*, 2(3), pp.213-228.
- Xu, X., Yang, Q., Yoshida, A. and Tamura, Y., 2017. Characteristics of pedestrian-level wind around super-tall buildings with various configurations. *Journal of Wind Engineering and Industrial Aerodynamics*, 166, pp.61-73
- Yoshie, R., Mochida, A., Tominaga, Y., Kataoka, H., Harimoto, K., Nozu, T. and Shirasawa, T., 2007. Cooperative project for CFD prediction of pedestrian wind environment in the Architectural Institute of Japan. *Journal of wind engineering and industrial aerodynamics*, 95(9-11), pp.1551-1578.
- Zhang, X., Weerasuriya, A. U., Lu, B., Tse, K. T., Liu, C. H., & Tamura, Y. (2020a). Pedestrian-level wind environment near a super-tall building with unconventional configurations in a regular urban area. In *Building Simulation* (Vol. 13, No. 2, pp. 439-456). Tsinghua University Press.
- Zhang, X., Weerasuriya, A. U., Zhang, X., Tse, K. T., Lu, B., Li, C. Y., & Liu, C. H. (2020b). Pedestrian wind comfort near a super-tall building with various configurations in an urban-like setting. In *Building Simulation* (Vol. 13, No. 6, pp. 1385-1408). Tsinghua University Press.